

# Identification of Residues in the C $\mu$ 4 Domain of Polymeric IgM Essential for Interaction with *Plasmodium falciparum* Erythrocyte Membrane Protein 1 (PfEMP1)<sup>1</sup>

Ashfaq Ghumra,<sup>2\*</sup> Jean-Philippe Semblat,<sup>2†</sup> Richard S. McIntosh,<sup>\*</sup> Ahmed Raza,<sup>†</sup> Ingunn B. Rasmussen,<sup>§</sup> Ranveig Braathen,<sup>‡§</sup> Finn-Eirik Johansen,<sup>‡</sup> Inger Sandlie,<sup>§</sup> Patricia K. Mongini,<sup>¶</sup> J. Alexandra Rowe,<sup>3†</sup> and Richard J. Pleass<sup>3\*</sup>

The binding of nonspecific human IgM to the surface of infected erythrocytes is important in rosetting, a major virulence factor in the pathogenesis of severe malaria due to *Plasmodium falciparum*, and IgM binding has also been implicated in placental malaria. Herein we have identified the IgM-binding parasite ligand from a virulent *P. falciparum* strain as PfEMP1 (TM284var1 variant), and localized the region within this PfEMP1 variant that binds IgM (DBL4 $\beta$  domain). We have used this parasite IgM-binding protein to investigate the interaction with human IgM. Interaction studies with domain-swapped Abs, IgM mutants, and anti-IgM mAbs showed that PfEMP1 binds to the Fc portion of the human IgM H chain and requires the IgM C $\mu$ 4 domain. Polymerization of IgM was shown to be crucial for the interaction because PfEMP1 binding did not occur with mutant monomeric IgM molecules. These results with PfEMP1 protein have physiological relevance because infected erythrocytes from strain TM284 and four other IgM-binding *P. falciparum* strains showed analogous results to those seen with the DBL4 $\beta$  domain. Detailed investigation of the PfEMP1 binding site on IgM showed that some of the critical amino acids in the IgM C $\mu$ 4 domain are equivalent to those regions of IgG and IgA recognized by Fc-binding proteins from bacteria, suggesting that this region of Ig molecules may be of major functional significance in host-microbe interactions. We have therefore shown that PfEMP1 is an Fc-binding protein of malaria parasites specific for polymeric human IgM, and that it shows functional similarities with Fc-binding proteins from pathogenic bacteria. *The Journal of Immunology*, 2008, 181: 1988–2000.

**I**mmunoglobulin M, the first Ab to be secreted during an immune response, is highly effective at neutralizing and agglutinating pathogens, and it also activates the classical complement cascade with a 1000-fold increased avidity than IgG (1). This increased avidity is largely due to the pentameric structure of IgM (2). A receptor for IgM (and IgA), the Fc $\alpha$ / $\mu$ R that is closely

related to the polymeric Ig receptor (pIgR)<sup>4</sup> in its ligand-binding domain, has recently been identified and shown to be expressed by a subset of B cells and macrophages, but not on granulocytes, T cells, or NK cells in the mouse spleen (3). The Fc $\alpha$ / $\mu$ R mediates endocytosis of IgM-coated bacteria and immune complexes and is thought to play a role in Ag processing and presentation during the primary stages of immunity (4, 5). Although parasite-specific IgM has been shown to play an important role in limiting parasite replication in rodent models of malaria, its role in human malaria remains largely undetermined (6, 7).

Natural IgM, produced by B-1 B cells of naive animals, has been identified as a link between innate and adaptive immune responses because of its ability to control the dissemination of both viruses and bacteria (8, 9). What role natural IgM plays in immunity to human malaria is less clear, although nonimmune IgM is known to bind to the surface of *Plasmodium falciparum*-infected erythrocytes, and it has been shown to correlate with rosetting and severe malaria in both laboratory strains and field isolates (10). Rosetting, the ability of infected erythrocytes to bind uninfected

\*Institute of Genetics, Queens Medical Centre, University of Nottingham, Nottingham, England, United Kingdom; †Institute of Immunology and Infection Research, School of Biological Sciences, University of Edinburgh, Edinburgh, Scotland, United Kingdom; ‡Institute for Pathology and Centre for Immune Regulation and §Department of Molecular Biosciences, University of Oslo, Oslo, Norway; and ¶Department of Rheumatology, Hospital for Joint Diseases, New York University Medical Center, New York, NY 10003

Received for publication April 24, 2008. Accepted for publication May 23, 2008.

The costs of publication of this article were defrayed in part by the payment of page charges. This article must therefore be hereby marked *advertisement* in accordance with 18 U.S.C. Section 1734 solely to indicate this fact.

<sup>1</sup> This work was supported by a Medical Research Council Career Establishment Award (G0300145) and a European Union Marie Curie Excellence Grant, Antibody Immunotherapy for Malaria (MEXT-CT-2003-509670) to R.J.P., A.R., J.-P.S., and J.A.R. were supported by a Wellcome Trust Senior Fellowship (grant no. 067431).

J.A.R. and R.J.P. share senior authorship. A.G. expressed recombinant DBL domains in bacteria, performed ELISAs, IFAs, and rosetting analysis, purified and characterized Ig domain swaps and mAbs, and generated IgM point mutants. J.-P.S. identified, cloned, and characterized the *TM284var1* gene and identified DBL4 $\beta$  as the IgM-binding ligand. R.S.M. helped with size-exclusion chromatography and domain swap culture and purification. A.R. cultured live rosetting parasite isolates and investigated IgM binding by IFAs. I.B.R., R.B., F.-E.J., and I.S. provided IgM domain-swapped expression plasmids, free secretory component, and important discussion. P.K.M. provided a panel of anti-IgM mAbs and contributed to discussion. J.A.R. and R.J.P. conceived and designed the overall study, provided laboratory facilities, and wrote the manuscript together.

<sup>2</sup> A.G. and J.-P.S. contributed equally to this work.

<sup>3</sup> Address correspondence and reprint requests to Dr. Richard J. Pleass, University of Nottingham, Institute of Genetics, Queen's Medical Centre, Nottingham NG7 2UH, England, U.K. E-mail address: richard.pleass@nottingham.ac.uk or Dr. Alexandra Rowe, Institute of Immunology and Infection Research, School of Biological Sciences, University of Edinburgh, West Mains Road, Edinburgh EH9 3JT, Scotland, U.K. E-mail address: alex.rowe@ed.ac.uk

<sup>4</sup> Abbreviations used in this paper: pIgR, polymeric Ig receptor; CIDR, cysteine-rich interdomain region; DAB, diaminobenzidine; DAPI, 4',6-diamidino-2-phenylindole; DBL, Duffy binding-like; IFA, immunofluorescent assay; NIP, 3-iodo-4-hydroxy-5-nitrophenacetyl; PfEMP1, *Plasmodium falciparum* erythrocyte membrane protein 1.

Copyright © 2008 by The American Association of Immunologists, Inc. 0022-1767/08/\$2.00

ones, is associated with severe malaria in African children (11, 12), and rosettes often contain nonspecific human IgM (13–16). Intriguingly, infected erythrocytes implicated in placental adhesion are also able to bind natural nonspecific IgM (17, 18). Although pathogenic parasite isolates clearly bind IgM, it is unclear what advantage the ability to bind IgM offers a parasite in an infected erythrocyte, although in the case of rosetting phenotypes, it has been suggested that IgM could act as a bridge between infected and uninfected erythrocytes to stabilize rosettes (14, 15). However, even in the absence of information concerning their exact biological role, the IgM binding proteins are of considerable interest as immunochemical tools and model systems. A similar situation prevails for the bacterial IgG-binding proteins staphylococcal protein A and streptococcal protein G, which have been extensively studied (19), but whose biological function is unknown.

The parasite ligands that mediate IgM binding have been shown to be members of the variant erythrocyte surface Ag family *P. falciparum* erythrocyte membrane protein 1 (PfEMP1), encoded by the *var* genes (20, 21). Every parasite contains 50–60 *var* genes in its genome, but only one is expressed at the surface of the infected erythrocyte (21). The *var* gene repertoires of different parasite isolates are largely nonoverlapping, resulting in extensive diversity in the PfEMP1 family (22). PfEMP1 molecules are composed of Duffy binding-like (DBL) domains classified into six types ( $\alpha$ ,  $\beta$ ,  $\gamma$ ,  $\delta$ ,  $\epsilon$ , and X), and cysteine-rich interdomain region domains (CIDR) classified into three types ( $\alpha$ ,  $\beta$ , and  $\gamma$ ) (23, 24). Individual *var* genes differ from each other by the number and type of these domains. A number of different PfEMP1 domains from specific PfEMP1 variants have been shown to bind nonimmune IgM, including a CIDR from the *FCR3S1.2var1* variant (25), a DBL $\beta$  from the *TM284S2var1* variant (26), two DBL $\epsilon$  domains from *FCR3var1CSA* and *FCR3var2CSA* variants (27), and one DBL-X and two DBL $\epsilon$  domains from *3D7var2CSA* (18). The precise binding sites for IgM within these domains are unknown, and there is no obvious motif shared by these domains that is missing from equivalent domains lacking IgM-binding function. It is also unknown which region of the IgM molecule is bound by PfEMP1, and whether different IgM-binding PfEMP1 variants bind similar or different regions of the IgM molecule.

Herein, we identify a new PfEMP1 variant as the IgM-binding ligand from a virulent *P. falciparum* strain derived from a patient with cerebral malaria, and we report experiments analyzing the interaction between IgM and PfEMP1. Using domain-swapped Abs, mutant IgM molecules, and specific mAbs to IgM, we show that PfEMP1 binding requires the C $\mu$ 4 domain of the IgM H chain, and that IgM polymerization is essential for binding by PfEMP1. Additionally, we found that one region of C $\mu$ 4 involved in PfEMP1 binding is homologous to the regions in IgG and IgA that are bound by bacterial Fc-binding proteins. Furthermore, using mAbs to the IgM C $\mu$ 3 and C $\mu$ 4 domains, we show that multiple *P. falciparum* strains implicated in both severe childhood and pregnancy-associated malaria use the same binding site on IgM.

## Materials and Methods

### Parasite culture and selection

Parasites were cultured in group O erythrocytes in RPMI 1640 medium supplemented with gentamicin, HEPES, glucose, and 10% pooled human serum as described previously (28). The parasite lines used were rosetting strains TM284 (29) and HB3R+, and the CSA-binding strains FCR3CSA, 202-CSA, and HB3-CSA (17). The TM284 strain used here is the parent of a parasite clone TM284S2 used in a previous study of Ig binding (26), and the PfEMP1 variant that we have identified (encoded by *TM284var1*) is distinct from that described by Flick et al. (*TM284S2var1*). Rosetting parasites were selected by plasmagel flotation (the upper phase contains only nonrosetting parasites and the lower phase contains rosetting parasites and

uninfected erythrocytes) (30). After staining an aliquot of parasite suspension with 25  $\mu$ g/ml ethidium bromide, rosette frequency (percentage of mature infected erythrocytes binding two or more uninfected erythrocytes) was assessed by fluorescence microscopy of a wet preparation.

### Immunofluorescence assays (IFAs) to detect normal human serum IgM binding to live infected erythrocytes

IFAs were conducted on mature trophozoite or schizont stage parasites grown in medium containing normal human serum as described previously (10), using a mouse mAb to human IgM (Serotec) diluted 1/1000 followed by incubation with Alexa Fluor 488-labeled goat anti-mouse IgG (Molecular Probes) diluted 1/500 plus 1  $\mu$ g/ml of 4,6-diamidino-2-phenylindole (DAPI, to stain the parasite nucleic acid and allow identification of infected erythrocytes). Controls were performed using secondary Ab/DAPI only. Parasite cultures were smeared on a slide and viewed under a fluorescent microscope.

### Protein extraction and immunoprecipitation assay

At late trophozoite stage, infected erythrocytes were washed twice in incomplete media (supplemented RPMI 1640 as described above, but lacking 10% serum) and half of the culture was treated with trypsin (100  $\mu$ g/ml) for 10 min at 37°C followed by the addition of soybean trypsin inhibitor (100  $\mu$ g/ml) for 10 min at 37°C. Proteins were extracted using a solution of 150 mM NaCl, 5 mM EDTA, 50 mM Tris-HCl (pH 8.0), and 1% Triton X-100 (NETT) containing one tablet of a cocktail of protease inhibitors (Roche) per 10 ml NETT. After centrifugation (10 min at 13,000 rpm, 4°C) the supernatant (Triton X-100 soluble fraction) was removed and used for immunoprecipitation. Pull-down assays were performed using 300  $\mu$ l of Triton X-100 soluble fraction mixed with 100  $\mu$ l of 10% slurry of protein L or protein G beads in NETT for 1 h on a Spiramix mixer at 4°C. Beads were washed twice in NETT/1% BSA, once in NETT/350 mM NaCl, twice in NETT, and once in Tris-saline (150 mM NaCl, 50 mM Tris-HCl (pH 8.0)). Beads were heated at 70°C in loading buffer and pelleted by centrifugation. The supernatant was analyzed on a NuPAGE Novex 3–8% Tris-acetate acrylamide gel (Invitrogen), transferred to polyvinylidene difluoride membranes, and blocked in PBS containing 5% skimmed milk. Membranes were probed with a 1/1000 dilution of mAb 6H1 (specific for the conserved intracellular portion of PfEMP1 (ref 28), a kind gift from S. Rogerson) followed by 1/1000 dilution of HRP-conjugated sheep anti-mouse IgG (Chemicon International), and the signal was developed using ECL Plus Western blotting detection reagents as described by the manufacturer (Amersham Biosciences).

### RNA extraction and *var* gene RT-PCR

TM284 parasites were divided into isogenic rosetting and nonrosetting subpopulations as described previously (30), and RNA was extracted from late ring-stage parasites using TRIzol (31). RNA (2  $\mu$ g) was used for cDNA preparation using SuperScript III kit (Invitrogen) according to the manufacturer's protocol. Briefly, after DNase I treatment for 30 min at room temperature, cDNA was synthesized using random hexamers. Central DBL $\alpha$  domain was amplified by PCR with degenerate primers using AmpliTaq Gold polymerase as described (32). PCR products were cloned into the PCR II vector (Invitrogen) and used to transform competent cells, and miniprep DNA was prepared from white colonies and sequenced as described previously (33).

### Sequencing of the *TM284var1* gene

A *var* gene (*TM284var1*) was identified that comprised the majority of *var* gene sequences derived from the TM284 rosetting parasites but was not detected in the set of *var* gene sequences derived from the TM284 nonrosetting parasites. The full-length sequence of *TM284var1* was obtained by a PCR-walking strategy using vectorette libraries (30).

### Northern blotting

RNA (1.5  $\mu$ g) in formamide loading buffer was loaded on a 1.2% agarose/1.1% formaldehyde gel, electrophoresed for 2 h at 150 V in 1 $\times$  MOPS running buffer, stained with 0.5  $\mu$ g/ml ethidium bromide for visualization, and transferred overnight onto a nitrocellulose membrane (Roche). Probe fragments were amplified from genomic DNA using AmpliTaq DNA polymerase and cloned into pCRII vector (Invitrogen). Primer sequences were as follows: DBL4 $\beta$  probe, forward 5'-tctctgcagctgaagatgaatggattgtaac-3', reverse 5'-acgagtgggcccatgtgaatcatcaatagg-3'; exon II probe: forward 5'-aaaaacaaaagcatctgttgaaattat-3', reverse 5'-gtgtgtttcactagtagtac-3'. Inserts were reamplified using Pfx DNA polymerase (Invitrogen), M13 reverse primer, and the forward primer of the insert. RNA probes

were synthesized from the PCR product using Sp6 RNA polymerase using the DIG Northern starter kit (Roche) according to the manufacturer's conditions. Blots were prehybridized for 1 h in DIG Easy buffer and probed overnight with 2  $\mu$ l of probe in 7 ml of DIG easy buffer at 58°C for the DBL4 $\beta$  probe or 52°C for the exon II probe. Membranes were washed for 45 min with 0.5 $\times$  SSC, 0.1% SDS followed by 45 min incubation in 0.25 $\times$  SSC, 0.1% SDS. Both incubations were performed at 62°C for the DBL4 $\beta$  probe or 55°C for the exon II probe. Membranes were incubated with 1/100 dilution of anti-Dig Ab before chemiluminescent detection with CDP-Star (Roche) as described by the supplier.

#### Expression of *TM284var1* domains in COS-7 cells

All PfEMP1 extracellular domains encoded by *TM284var1* were PCR amplified and cloned into the pRE4 expression vector using *PvuII*-*ApaI* restriction sites as described previously (27, 34, 35). The amino acid boundaries of the constructs were as follows: DBL1 $\alpha$  (82–422), CIDR $\beta$  (455–674), DBL2 $\gamma$  (749–1100), DBL3 $\epsilon$  (1082–1499), DBL4 $\beta$  (1481–1952), and DBL5 $\epsilon$  (1914–2285). The primers used were: DBL1 $\alpha$ , 5'-tctctgacgtgggataaccaccgcaagg-3' and 5'-acgagtgccctgtgactaaaattctg-3'; CIDR $\beta$ , 5'-tctctgacgtgtctgctgtattgtgtg-3' and 5'-acgagtgccctcattgacttcccaattg-3'; DBL2 $\gamma$ , 5'-tctctgacgtggacaaaactgtttcaagt-3' and 5'-acgagtgccctcttcttctggtgtatcg-3'; DBL3 $\epsilon$ , 5'-tctctgacgtgacagactatgatacaaatgc-3' and 5'-acgagtgccctggatgatattgtggcttc-3'; DBL4 $\beta$ , 5'-tctctgacgtggagatcaactacag-3' and 5'-acgagtgcccgactaacccgactagg-3'; DBL5 $\epsilon$ , 5'-tctctgacgtggagtgtaacgaactaacactg-3' and 5'-acgagtgccccaatgagacaatcaattac-3'. PCR conditions were as follows: 3 min at 94°C followed by 3 cycles: 94°C for 30 s, 45°C for 30 s, and 60°C for 1.5 min; 3 cycles: 94°C for 30 s, 48°C for 30 s, and 60°C for 1.5 min; and 24 cycles: 94°C for 30 s, 50°C for 30 s, and 60°C for 1.5 min. The pRE4 vector contains the herpes simplex glycoprotein D signal sequence fused to the DBL domain of interest and a transmembrane signal sequence targeting the fusion protein to the surface of transfected COS-7 cells. COS-7 cells were transiently transfected with 1  $\mu$ g of DNA using 3  $\mu$ l of FuGENE 6 as described by the manufacturer (Roche). Transfection efficiency and ability to bind IgM were assessed by IFA with mAbs DL6 and anti-human IgM, respectively, as described before (27).

#### Bacterial expression of PfEMP1 domains

Bacterial expression of PfEMP1 domains was conducted by modification of the methods of Singh et al. (36). A PCR product containing a His-tagged DBL4 $\beta$  domain was subcloned as a *NheI*-*XhoI* fragment into the bacterial expression vector pET28a (Novagen) using the following sets of primers: 5'-ctagctagcgaagagctcaatactacag-3' and 5'-ccgctcagagtaacatcccgagtagg-3' and transformed into the *Escherichia coli* BL21 Rosetta strain. Protein expression was induced by isopropyl- $\beta$ -D-1-thiogalactopyranoside (IPTG) and bacterial pellets lysed in BugBuster (Novagen) containing protease inhibitors (Roche). Inclusion bodies were washed twice in 50 ml of 50 mM Tris-HCl (pH 7.4) containing 500 mM NaCl, 2 M urea, 1 mM EDTA, and 0.1% Igepal CA-630 (Sigma-Aldrich) with a final wash in double-distilled H<sub>2</sub>O. Bacterial pellets were then denatured in 50 ml 8 M urea before the addition of 5 ml of Talon metal affinity resin (Clontech) and rolled overnight at room temperature to allow binding. Bound protein was washed and eluted with 300 mM imidazole according to the manufacturer's instruction and renatured into PBS using stepwise dialysis with reducing concentrations of urea at 4°C. Protein concentrations were determined by a bicinchoninic acid assay (Pierce) and purity assessed by SDS-PAGE on 12% bis-Tris polyacrylamide gels stained with SimplyBlue (Invitrogen) or by immunoblotting with anti-His-HRP (Sigma-Aldrich).

#### Abs: domain swap, point mutants, and controls

IgM/IgG and IgM/IgA1 domain-swapped, point-mutant, and IgG1 or IgA1 Abs specific for the hapten NIP (3-iodo-4-hydroxy-5-nitrophenyl) were purified from tissue culture supernatants as previously described (37–41). Other Abs used for investigating binding to PfEMP1 were obtained from commercial sources as follows: human IgA2 and IgM anti-NIP (Serotec), mouse IgM $\lambda$  (BD Pharmingen) and IgM Fab $\mu$  fragment (Rockland). Detecting Abs used in ELISAs and IFAs include anti-polyhistidine-HRP mAb (HIS-1, Sigma-Aldrich); goat anti-mouse  $\lambda$ -RPE (Southern Biotechnology Associates); goat anti-mouse  $\lambda$ -biotin (Southern Biotechnology Associates); mouse mAb DL6 anti-HSV-1 gD (Santa Cruz Biotechnology); goat anti-mouse IgG Fab-FITC (Sigma-Aldrich); goat F(ab')<sub>2</sub> anti-human IgM Fc $\mu$ -RPE (Caltag Laboratories); mouse anti-human IgM  $\kappa$ -chain specific (Sigma-Aldrich); and goat anti-human IgM  $\mu$ -chain specific-HRP (Sigma-Aldrich). A panel of anti-IgM  $\mu$ -chain-specific mAbs used in blocking studies (1F11, 4-3, 1G6, 5D7, 196.6b, HB57, 1X11) have been described previously (42, 43).

The anti-C $\mu$ 4-specific mAb 2F11 was kindly provided by Professor Tor Lea (Institute of Immunology, Rikshospitalet, Oslo, Norway).

#### Construction of IgM mutants

The C $\mu$ 4 domain IgM mutants NR445–446HL and PLSP394–397LLPQ were constructed using site-directed mutagenesis (QuickChange II XL kit; Stratagene) using the following forward and reverse primer sets (5'-catgaggccctgccccactggtcaaccgagaggac-3' and 5'-gtcctctcgtgaccaggtggcgaggccctcatg-3' for IgM NR445–446HL, and 5'-gcagagggggcagctctgcccaggagaagtatgga-3' and 5'-tcacatactctctgggcaagagctgccccctctgc-3' for IgM PLSP394–397LLPQ, all from MWG Biotech) on the wild-type pSV2gptV<sub>NP</sub> IgM plasmid using PCR (37). To verify incorporation of the desired mutations and to check for PCR-induced errors, the entire  $\mu$  H chain regions of all the expression vectors were sequenced. The mutant H chain genes were transfected by electroporation into the murine myeloma cell line J558L (European Collection of Cell Cultures), constitutively producing a mouse  $\lambda$ 1 L chain and a J chain, but no Ig H chains. The cells were grown in RPMI 1640 medium supplemented with 10% FCS, 100 IU/ml penicillin, and 100  $\mu$ g/ml streptomycin (Invitrogen) at 37°C/5% CO<sub>2</sub>. Stable transfectants were selected in medium containing 250  $\mu$ g/ml xanthine and 1  $\mu$ g/ml mycophenolic acid and IgM-positive colonies selected by ELISAs on supernatants using NIP-BSA (Bioserch Technologies) coated microtiter wells as previously described (41).

#### Analysis of domain-swapped Abs binding to PfEMP1 domains by ELISA

Nunc MaxiSorp microtiter plates, coated overnight with 5  $\mu$ g/ml purified Ab in coating buffer (0.05 M sodium carbonate (pH 9.6)), were blocked with PBS containing 5% milk powder and 0.1% (v/v) Tween 20. All Abs used to coat wells were of equal concentration as determined by the bicinchoninic acid assay and anti-NIP ELISAs with goat anti-mouse  $\lambda$ -biotin and streptavidin-HRP (Serotec). After three washes with PBS, 50  $\mu$ l of varying concentrations of DBL4 $\beta$  was added in PBS containing 1% milk powder and Tween 20 as above (PBSMT) to duplicate wells and incubated for 2 h at room temperature before washing as above. In blocking experiments, wells coated with IgM were incubated with varying concentrations of anti-IgM mAbs for 1 h before the addition of DBL4 $\beta$ . Bound DBL4 $\beta$  was detected using anti-His-HRP (Sigma-Aldrich) at 1/1000 in PBSMT and incubated for 1 h. After washing as above, reactions were developed by incubating with substrate (Sigma-Aldrich 3,3',5,5'-tetramethylbenzidine dihydrochloride tablets made up according to the manufacturer's instructions).

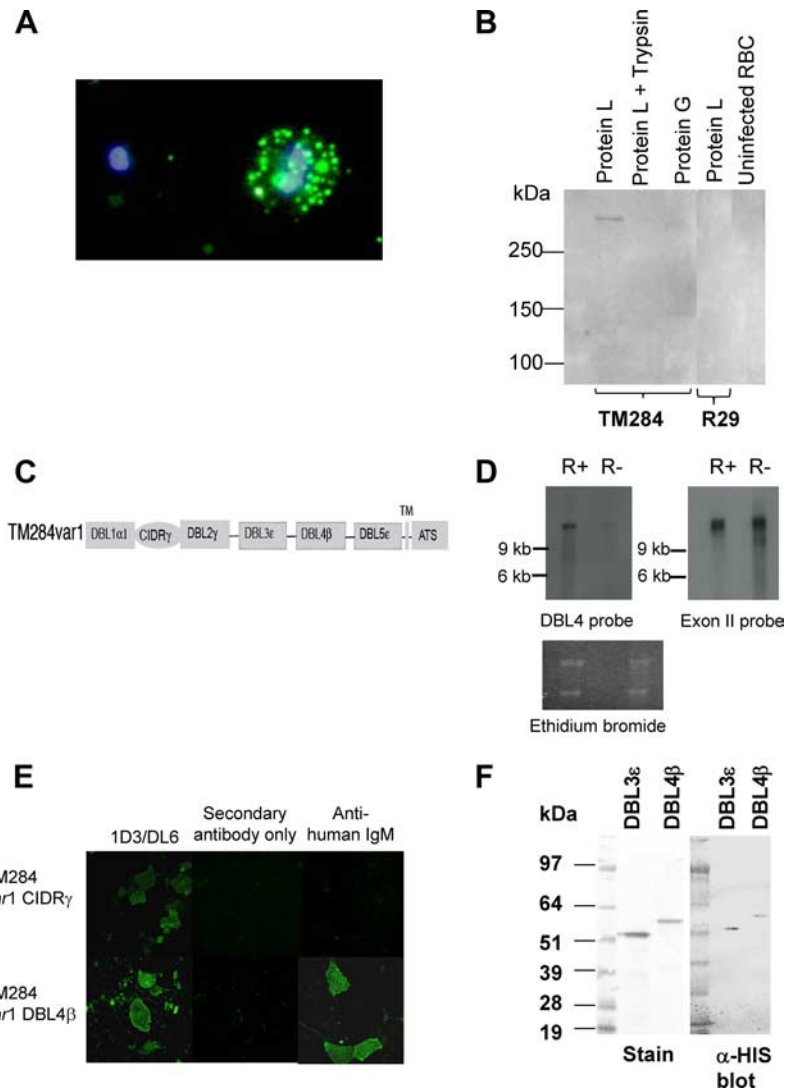
#### Analysis of domain-swapped Abs binding to PfEMP1 domains expressed in COS-7 cells by IFA

DBL4 $\beta$  and DBL5 $\epsilon$  domains from *TM284var1* transiently expressed on the surface of COS-7 cells (as above) were grown on the surface of 12-mm circular coverslips (Raymond A Lamb). Cells were washed in PBS and fixed in ice cold 50/50 methanol acetone solution for 20 min. After washing in PBS, cells were blocked in PBS/5% FCS for 1 h. After washing, 2 ng mAb DL6 to detect the glycoprotein D tag as a marker of transfection efficiency, and 10 ng of Ab in a final volume of 50  $\mu$ l PBS/1% FCS, was spotted onto parafilm and laid on top of each cover slip for 1 h in a humid chamber. For blocking experiments, IgM was preincubated with varying concentrations of anti-IgM mAb for 1 h before incubation with DBL transfectants. Cells were washed three times in PBS/1% FCS before the addition of a 1/100 dilution of goat anti-mouse IgG-FITC and goat anti-mouse  $\lambda$ -RPE for 1 h in the dark. Cells were washed as above with a final wash in PBS and mounted with ProLong Gold antifade reagent containing DAPI (Invitrogen) and viewed by fluorescence microscopy.

#### IFAs of live infected erythrocytes with domain-swapped Abs

To prevent the binding of native IgM from the culture medium, parasites were grown in medium with 10% IgM-depleted human serum, obtained by three sequential incubations of human serum with anti-human IgM linked to agarose beads (Sigma-Aldrich). Western blotting with an anti-human IgM Ab confirmed the complete removal of IgM from human serum following this procedure (data not shown). The binding of domain-swapped Abs to infected erythrocytes (see Tables II and III) was as described previously with minor modifications (17). Briefly, 50- $\mu$ l aliquots of parasite cultures at 2% hematocrit were washed in PBS and resuspended in PBS containing 1% Ig-free BSA (Sigma-Aldrich) (PBS-BSA). Abs (1.6  $\mu$ g) were added to each aliquot and cultures were incubated on ice for 1 h. Cells were washed twice with PBS-BSA and resuspended in 1/200 dilution of goat anti-mouse  $\lambda$ -FITC (Caltag Laboratories) in PBS-BSA containing 50 ng DAPI. After a further incubation for 1 h and washes as above, cells were

**FIGURE 1.** Characterization of *TM284var1* and expression of recombinant DBL domains. **A**, IFA on live *TM284*-infected erythrocytes using mouse anti-human IgM (1/1000) and Alexa Fluor 488-conjugated goat anti-mouse secondary Abs (1/500). An IgM-positive rosetting infected erythrocyte shows punctuate surface fluorescence, while a nonrosetting infected erythrocyte is negative. Parasite nuclei stained with DAPI. **B**, Protein extracts from *TM284* or *IT/R29* parasites, in the presence or absence of trypsin, were incubated with either protein L (to pull out IgM) or protein G (to pull out IgG) beads. Immunoprecipitated products were run on 3–8% acrylamide Tris-acetate gels and transferred to polyvinylidene difluoride membranes for blotting with the anti-PfEMP1 mAb 6H1. The product at >250 kDa represents PfEMP1. **C**, Domain structure of the PfEMP1 variant encoded by the *TM284var1* gene. **D**, Northern blot of ring-stage rosetting (R+) and nonrosetting (R-) *TM284* parasites probed with a *DBL4β* probe specific for *TM284var1* (left panel) or an exon II probe recognizing all *var* genes (right panel). Ethidium bromide-stained gel is shown as an indication of loading (lower panel). Bars indicate the position of the 9-kb and 6-kb bands of the RNA Millennium markers (Ambion). **E**, IFA on COS-7 cells transfected with *TM284 var1CIDRβ* (upper panel) and *TM284 var1DBL4β* (lower panel). COS-7 cells were incubated with mAbs 1D3 or DL6 to determine transfection efficiency (left column), with secondary Ab alone as negative control (middle column) or with mouse mAb to human IgM (right column). **F**, Western blot analysis of purified DBL domains of *TM284var1* expressed in *E. coli*. Polyvinylidene difluoride membranes were incubated with peroxidase conjugated anti-His as described in *Materials and Methods*. An equivalent SimplyBlue-stained SDS-PAGE 4–15% gradient gel is shown on the left; 2 μg of protein was loaded per lane.



resuspended in a 1/1000 dilution of chicken anti-goat Ig-Alexa Fluor 488 (Invitrogen). After another set of incubations and washes, cells were resuspended at 30% hematocrit in PBS-BSA and smeared on slides for immunofluorescence microscopy.

#### IFAs of live infected erythrocytes with IgM-specific blocking mAbs

Parasites were grown in IgM-depleted human serum as described above. Five micrograms of anti-NIP human IgM (Serotec) was incubated for 12 h at 4°C with 12 μg of the IgM-specific mAbs IX11 (*Cμ1* specific), 4-3 (*Cμ3* specific), and IF11 (*Cμ4* specific). The IgM/blocking mAb mixture was then incubated with live parasites and IFA conducted as described above for the domain-swapped Abs.

#### “Pseudo”-rosetting assays

Human erythrocytes were derivatized with NIP and sensitized with varying concentrations of IgM, IgA1, or the  $\alpha$ /*Cμ4* domain-swapped Ab (41). Coating levels for each Ab were found to be equivalent by reactivity with anti- $\lambda$  L chain-FITC as assessed by flow cytometry (data not shown). COS-7 transfectants were washed twice in PBS and resuspended at  $1 \times 10^6$  cells/ml. Rosetting of sensitized erythrocytes to *DBL4β*-transfected COS-7 cells was performed as previously described (41). To investigate the effects of complement at disrupting rosette formation, IgM-coated (20 μg/ml) erythrocytes were incubated with C1q (100 μg/ml, Sigma-Aldrich) or a 1/200 dilution of serum/plasma in barbitone complement fixation test diluent supplemented with 0.1% gelatin and 0.5% BSA (Veronal buffer; Oxoid). Binding of C1q to IgM-opsonized erythrocytes was confirmed by IFA with anti-C1q conjugated to FITC (Serotec). After 1 h incubation of eryth-

rocytes in serum, a 1/10 dilution of the anti-*Cμ4* mAb 4-3 was added for an additional 1 h before incubation with the *DBL4β* transfectants. A pseudo-rosette was defined as a transfected COS-7 cell surrounded by five or more opsonized erythrocytes.

## Results

### Identification of PfEMP1 as the IgM-binding ligand from the *TM284* strain

*TM284* is a *P. falciparum* rosetting strain that shows strong binding to human IgM when grown in culture medium containing pooled naive human serum (10, 14) (Fig. 1A). To identify whether

Table I. *M284var1* domains and their ability to bind human IgM

Domain	Transfection Efficiency (%) <sup>a,b</sup>	IgM Binding (%) <sup>b,c</sup>
DBL1 $\alpha$	5–10	0
CIDR $\beta$	20–25	0
DBL2 $\gamma$	15–20	0
DBL3 $\epsilon$	5–10	0
DBL4 $\beta$	10–15	8–12
DBL5 $\epsilon$	15–20	0

<sup>a</sup> Transfection efficiency was calculated by IFA using mAb DL6.

<sup>b</sup> Data from at least three experiments for each domain are shown.

<sup>c</sup> IgM binding was determined by IFA using a mouse anti-human IgM mAb.

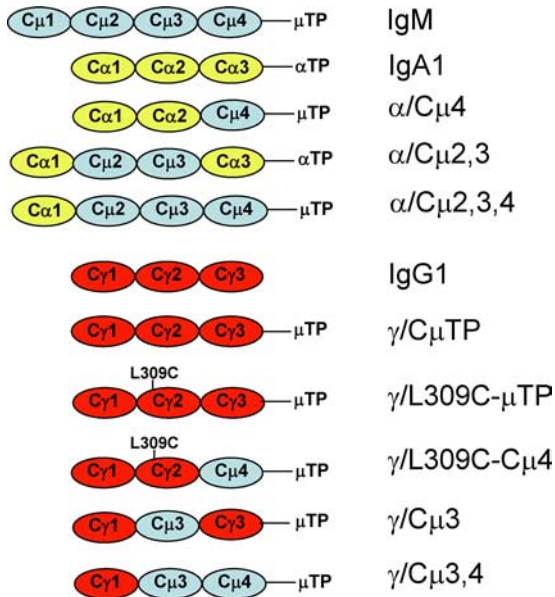


**FIGURE 2.** Overview of Ab H chain constructs. Constant H chain domains/sequences are shown as blue ( $\mu$ ), yellow ( $\alpha$ ), or red ( $\gamma$ ) ovals. TP indicates secretory tailpiece. L309C marks a single amino acid replacement of the leucine from IgG to the cysteine from the homologous position in IgM, to create a domain-swapped Ab with greater ability to polymerize (38).

PfEMP1 was the parasite ligand responsible for IgM binding, we conducted immunoprecipitation experiments using protein L-sepharose beads on Triton X-100-soluble protein extracts from

the TM284 strain (Fig. 1B). A high-molecular mass (>250 kDa), trypsin-sensitive protein was immunoprecipitated that could be blotted with mAb 6H1 recognizing the well-conserved intracellular domain of PfEMP1 (44). Control immunoprecipitations with protein G (that binds IgG but not IgM) failed to precipitate a similar-sized molecule, and no product was detectable with the other controls, including the non-IgM-binding IT/R29 parasite strain (10) or uninfected erythrocytes. Taken together, these results indicate that a PfEMP1 variant expressed by TM284 binds human IgM but not IgG.

*Characterization of the TM284var1 gene*

To allow detailed investigation of the molecular interactions between PfEMP1 and human IgM, we cloned and sequenced the *var* gene encoding the predominant PfEMP1 variant expressed by TM284 rosetting parasites. TM284 was selected to high rosette frequency (>70% of infected erythrocytes in rosettes) and then separated into rosetting and nonrosetting subpopulations (30). RNA was extracted from each subpopulation and RT-PCR performed using degenerate primers to the *var* gene DBL $\alpha$  domain (32). The resulting PCR products were cloned and sequenced, and the predominantly transcribed gene from the rosetting parasites, which was absent from the nonrosetting parasites, was identified as *TM284var1*. The full-length *TM284var1* gene was cloned and sequenced by PCR walking using vectorette libraries (30). Analysis of the full sequence indicated that *TM284var1* encodes a PfEMP1 variant containing six extracellular domains (Fig. 1C), plus a transmembrane domain and the intracellular acidic terminal sequence. The upstream sequence of *TM284var1* is of the UpsA type (23),

**FIGURE 3.** Binding of IgA/IgM and IgG/IgM domain swaps to DBL domains. ELISA analysis of recombinant DBL4 $\beta$  from the TM284var1 variant binding to IgA/IgM (A) or IgG/IgM (B) domain-swapped Abs immobilized in microtiter wells (left panels). No binding was seen with control DBL3 $\epsilon$  (R29var1 variant) (30) or DBL5 $\epsilon$  (Tm284var1 variant) in the same ELISA. Binding of domain-swapped Abs was also investigated by IFA with COS-7 cells expressing DBL4 $\beta$  or DBL5/3 $\epsilon$  (right panels). Positive transfectants were detected with mAb DL6 reactive with the HSV-glycoprotein D tag expressed C-terminally of the DBL domain. DL6 was then detected with a FITC-labeled anti-mouse IgG (green). Binding of domain-swapped Abs was detected with a PE-labeled anti-mouse  $\lambda$  (red) that binds to the common L chain shared by all the domain-swapped Abs. Only transfected cells incubated with IgM,  $\alpha$ /C $\mu$ 2,3,4,  $\alpha$ /C $\mu$ 4,  $\gamma$ /L309C-C $\mu$ 4, and  $\gamma$ /C $\mu$ 3,4 bound DBL4 $\beta$  by IFA, and this recapitulated data seen by ELISA. Binding of domain-swapped Abs colocalized with DBL4 $\beta$  seen on the surface of unfixed COS-7 cells (C). No binding of Abs was seen to control COS-7 cells expressing either DBL3 $\epsilon$  or DBL5 $\epsilon$ .

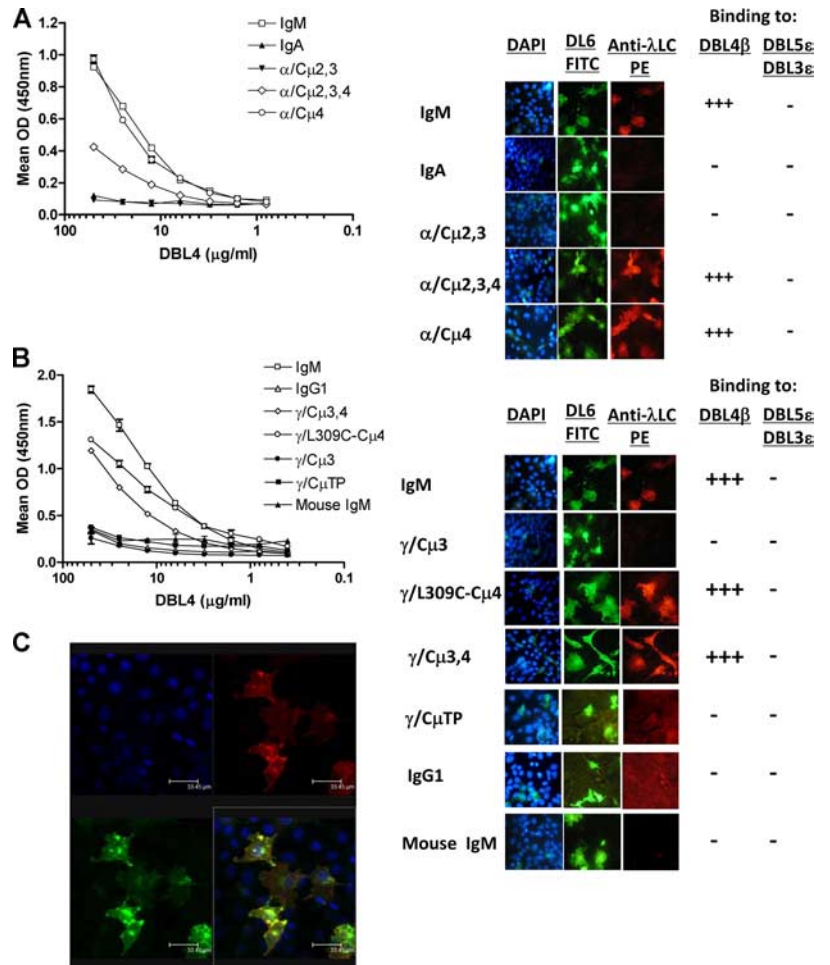


Table II. Binding of recombinant domain-swapped Abs to infected erythrocytes<sup>a</sup>

Antibody	Parasite Strain	
	TM284	FCR3CSA
Human IgM	+++	+++
Human IgG1	—	—
Human IgA1	—	—
Mouse IgM <sup>b</sup>	—	—
Human IgM Fab	—	—
γ/Cμ3,4	++	++
γ/L309C-Cμ4	+/-	++
γ/Cμ3	—	—
γ/CμTP	—	—
IgM C575S (monomeric IgM)	—	—
γ/L309C-μTP (polymeric IgG)	—	—
α/Cμ2,3	—	—
α/Cμ2,3,4	++	++
α/Cμ4	++/-	++

<sup>a</sup> Data representing results from two or more experiments are summarized for simplicity. Positive cells showed punctate green fluorescence over the surface of infected erythrocytes as shown in Fig 1A. +++, ≥50% of infected erythrocytes positive; ++, 20–40% of infected erythrocytes positive; +, 10–20% of infected erythrocytes positive; —, no infected erythrocytes positive.

<sup>b</sup> Mouse IgM also failed to bind to HB3R+ (rosetting) and HB3CSA, 202CSA (CSA-binding) parasite isolates.

indicating that *TM284var1* is a group A *var* gene, a subgroup that is associated with rosetting and is implicated in the pathogenesis of the most life-threatening forms of malaria (33, 45, 46). To confirm that *TM284var1* is the predominantly transcribed *var* gene from TM284 rosetting parasites, a Northern blot of RNA extracts from TM284 rosetting and nonrosetting subpopulations was probed with an anti-DBL4β probe specific for *TM284var1*. A strong signal was obtained only in the TM284 rosetting population (Fig. 1D). A probe to the *var* gene exon 2, encoding the conserved acidic terminal sequence region, that detects many/all *var* genes was also used and showed that the nonrosetting parasites transcribe other *var* genes (Fig. 1D).

Additional evidence that *TM284var1* encodes the predominant IgM-binding, rosette-mediating PfEMP1 variant comes from a selection experiment in which IgM-binding TM284-infected erythrocytes were FACS sorted to enrich for IgM-positive cells, and then returned to culture. The starting culture was low rosetting and low IgM binding (20%). After FACS sorting for IgM-positive cells and culturing for 2 wk (necessary to produce enough material for

experiments), the culture was 88% rosetting and IgM binding, and a repeat of the RT-PCR confirmed that the predominantly transcribed *var* gene was *TM284var1* (data not shown). Therefore, selection for IgM binding increases rosetting and selects for parasites transcribing the *TM284var1* gene.

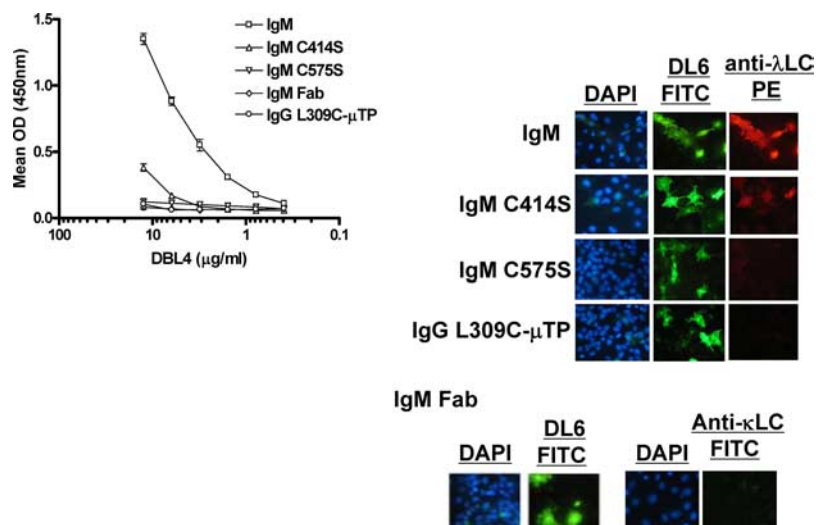
*Identification of DBL4β as the IgM-binding domain of the TM284var1 PfEMP1 variant*

To identify the IgM-binding domain of *TM284var1*, each DBL and CIDR domain was cloned into the pRE4 expression vector and expressed at the surface of COS-7 cells (34). Transfection efficiency for each construct was determined by IFA with mAb DL6 specific for the HSV-glycoprotein D epitope expressed C-terminally to each PfEMP1 domain as part of the pRE4 vector (35). IgM binding was detected by IFA using a mouse mAb to human IgM after incubation of the transfected COS cells in human serum. The level of expression for all domains ranged from 5 to 25% (Table I). DBL4β was identified as the domain from *TM284var1* that binds human IgM (Fig. 1E and Table I). The DBL4β domain is composed of 291 amino acids including 12 cysteine residues. Phylogenetic comparison with other DBLβ domains showed that *TM284var1* DBL4β clusters with domains called “β2” that differ from other DBLβ domains at the nucleotide level and are also characterized by the absence of a PfEMP1 C2 domain, which occurs after β1-type domains and plays an important role in their function (24).

*Bacterial expression of a soluble DBL4β domain*

Since the DBL4β domain of *TM284var1* uniquely bound human IgM (Table I), we expressed this domain as a His-tagged protein in *E. coli* to allow further characterization of IgM-PfEMP1 interactions. The recombinant *TM284var1* DBL4β domain expressed in *E. coli* accumulated in inclusion bodies as seen for other DBL domains (36). The protein was extracted and refolded using 8 M urea and methods similar to those described previously (36). The final yield of refolded and purified protein from shaken flask cultures was ~1 mg/L. The purified DBL4β protein runs as a monomer at ~55 kDa on both reducing and nonreducing SDS-PAGE gradient gels, in line with the expected molecular mass of 55.734 kDa determined by ProtParam (<http://www.expasy.ch/tools/protparam.html>) and confirmed by immunoblotting with anti-His-HRP (Fig. 1F). We also expressed in an identical manner two non-IgM-binding DBL domains to act as controls in

FIGURE 4. The polymerization status of IgM is crucial for binding to DBL domains. Anti-NIP recombinant human IgM and various point mutants deficient in polymerization (IgM C414S and IgM C575S) were examined for binding to DBL4β by ELISA (left panel) and by IFAs (right panel) as described for Fig. 3. A reduced binding was seen for IgM C414S, and no binding was seen with IgM C575S. IgM Fabs or polymeric IgG (IgG L309C-μTP) showed no binding when used at equivalent molar concentrations to IgM in both assays.



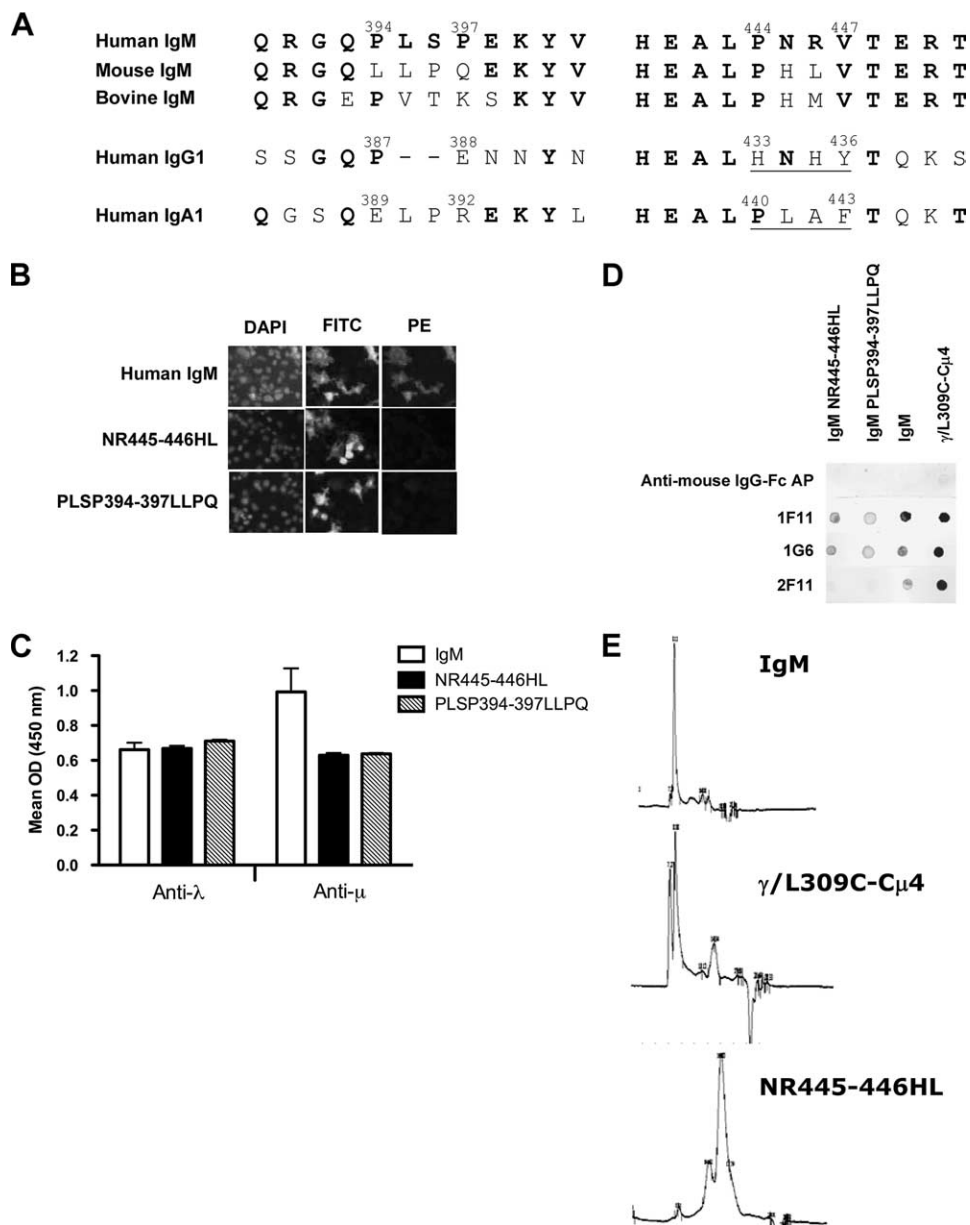


**FIGURE 5.** Localization of the DBL4 $\beta$  binding site in the C $\mu$ 4 domain of IgM. *A*, Amino acid alignment of human, mouse, and bovine IgM with human IgA1 and IgG1 at two exposed interdomain loop regions within the C $\mu$ 4 domain (see Fig. 8*B*). The IgA1 or IgM sequences are numbered according to the commonly adopted schemes used for IgA1 Bur (59) or IgM (60), whereas Eu numbering is used for IgG (61). Residues set in boldface type are conserved between species. Human IgG1 and IgA1 residues involved in contact with protein A and Fc $\alpha$ R (CD89), respectively, are underlined (41, 49). *B*, Binding of anti-NIP human IgM and the C $\mu$ 4 mutants NR445-446HL and PLSP394-397LLPQ were examined for binding to DBL4 $\beta$  by IFA as described for Fig. 3. Neither mutant was seen to bind DBL4 $\beta$ . *C*, Binding and detection of IgM point mutants to NIP-BSA immobilized onto microtiter plates. Abs were detected with peroxidase-conjugated anti- $\lambda$  of anti- $\mu$  as described in *Materials and Methods*. *D*, Epitope mapping of mAb binding to the IgM point mutants NR445-446HL and PLSP394-397LLPQ by immunoblotting. *E*, Size-exclusion chromatograms of recombinant human IgM,  $\gamma$ /L309C-C $\mu$ 4, and IgM NR445-446HL Abs run on a Superdex GL200 column.

functional experiments: DBL3 $\epsilon$  from the *IT/R29var1* variant and DBL5 $\epsilon$  (from *TM284var1*) (Ref. 27 and data not shown).

#### The *TM284var1* DBL4 $\beta$ domain of PfEMP1 binds to the Fc of IgM

To determine which part of the IgM molecule the *TM284var1* DBL4 $\beta$  domain binds, we used two panels of domain-swapped Abs (depicted in Fig. 2), in which homologous domains were exchanged between IgA/IgM (Fig. 2, upper panel) and IgG/IgM (Fig. 2, lower panel). These domain-swapped Abs consist of mouse L chain- and H chain-variable regions (specific for the hapten NIP) linked to human H chain-constant regions. The chimeric domain-swapped Abs were designated following these examples:  $\alpha$ /C $\mu$ 4 (constant domain structure C $\alpha$ 1C $\alpha$ 2C $\mu$ 4) and  $\gamma$ /C $\mu$ 3,4 (constant domain structure C $\gamma$ 1C $\mu$ 3C $\mu$ 4). Such Abs were composed of mixtures of both monomers and polymeric forms. Abs with the L309C mutation exist predominantly in higher polymeric forms, including pentamers and hexamers (see Fig. 5*E* and Refs. 37–39).

The ability of the recombinant *TM284var1* DBL4 $\beta$  domain to bind the domain-swapped Abs was analyzed by ELISA (Fig. 3, *A* and *B*,

left panels). We observed that only those domain-swapped Abs containing the  $\mu$ 4 constant domain were able to interact with soluble *TM284var1* DBL4 $\beta$  with an apparent affinity generally comparable to IgM (Fig. 3). In contrast, no binding was observed with human IgA, human IgG, mouse IgM, or domain swaps lacking the constant  $\mu$ 4 domain. As all these domain-swapped Abs share similar Fab regions and light chains and are epitope-matched for NIP, we can also deduce that the Fc region mediates all of the binding, a result confirmed by the observation that human IgM Fabs failed to bind (see Fig. 4 and below). No binding of any Ab was seen in ELISAs with recombinant *IT/R29var1* DBL3 $\epsilon$  or *TM284var1* DBL5 $\epsilon$  domains also expressed in *E. coli* (data not shown).

To confirm the results from recombinant protein expressed in *E. coli*, we also transiently expressed *TM284var1* DBL4 $\beta$  and DBL5 $\epsilon$  (negative control) domains in the pRE4 vector in mammalian COS-7 cells. Only cells expressing DBL4 $\beta$  bound IgM or domain swaps containing the C $\mu$ 4 domain, and they failed to bind control IgG or IgA, in a manner that recapitulated our findings with ELISA (Fig. 3, *A* and *B*, right panels). Confocal microscopy clearly showed that IgM binding co-localizes with the expressed

pRE4 tag and DBL4 $\beta$  domain, as witnessed by discrete punctate orange staining on the surface of the COS-7 cell (Fig. 3C), resembling the staining pattern seen with live parasites (Fig. 1A). No binding was seen with the control DBL5 $\epsilon$  domain from *TM284var1* despite equal transfection efficiencies as determined by the binding of mAb DL6 recognizing the pRE4 tag.

The requirement of the C $\mu$ 4 domain for IgM binding was repeated in IFA experiments on live parasites with the rosetting TM284 strain. The parasites were grown in IgM-depleted human serum to prevent the binding of native IgM, and then incubated with the various domain-swapped Abs. As seen with the *TM284var1* DBL4 $\beta$  domain expressed in either *E. coli* or COS-7 cells (Fig. 3), TM284 live infected erythrocytes only bound those domain swaps containing the C $\mu$ 4 domain (Table II). Furthermore, binding to a second IgM-binding parasite strain (FCR3CSA) expressing the *FCR3var2csa* variant (27), known to be implicated in pregnancy malaria (47), was also dependent on the C $\mu$ 4 domain of IgM (Table II). In contrast with the *FCR3var2csa* variant, the TM284 strain appeared to require contributions made by the C $\mu$ 3 domain, since those Abs uniquely containing the C $\mu$ 4 domain did not bind in two of the four experiments undertaken. Therefore, we show that two distinct *P. falciparum* strains have the ability to bind to the Fc of human IgM via the C $\mu$ 4 domain, and in the TM284 isolate this binding is mediated by PfEMP1.

#### Binding of PfEMP1 is dependent on the polymeric nature of IgM

We investigated whether the binding of *TM284var1* DBL4 $\beta$  is dependent on the ability of IgM to polymerize. We examined the binding of IgM point mutants with disrupted capability to polymerize and that are secreted from J558L cells principally as monomers (37–40). Two point mutants of IgM, one predominantly monomeric (IgM C575S) and one existing as 70% multimers/30% monomers (IgM C414S), were significantly reduced in their capacity to bind DBL4 $\beta$  (Fig. 4), in particular the IgM C575S mutant whose tailpiece cysteine (Cys<sup>575</sup>) is known to make a major contribution to polymerization, as mutation of this residue to serine or alanine leads to secretion of large amounts of monomers (47, 48). The monomeric form of IgM (C575S) also failed to bind to live infected erythrocytes by IFA (Table II), confirming that properties of whole infected erythrocytes are highly similar to those of the individual IgM-binding domain from the *TM284var1* PfEMP1 variant.

Polymerization was not, however, the only dictator of whether an Ab binds to PfEMP1, since  $\gamma$ L309C- $\mu$ TP, an IgG molecule in which the tailpiece of IgM had been attached to the C terminus, and thereby allowing the production of pentameric and hexameric forms of IgG, did not bind to either live parasites or recombinantly expressed *TM284var1* DBL4 $\beta$  (Fig. 4 and Table II). Furthermore, commercial polymeric murine IgM from two separate suppliers failed to bind in an experiment. Similarly, polymeric versions of IgA1 did not bind DBL4 $\beta$  (Fig. 3). Therefore, the above data show that the interaction of PfEMP1 with human IgM is dependent on both the primary amino acid sequence in the C $\mu$ 4 domain and the polymeric nature of IgM.

#### Identification of C $\mu$ 4 domain residues involved in DBL4 $\beta$ binding by IgM

Since we have shown a clear requirement for the C $\mu$ 4 domain of IgM in PfEMP1 binding, we chose to determine whether exposed residues in the C $\mu$ 4 domain might be directly involved in the interaction with *TM284var1* DBL4 $\beta$ . We generated two IgM Abs, each with amino acid substitutions in either of two exposed loops, comprising Pro<sup>394</sup>-Pro<sup>397</sup> and Pro<sup>444</sup>-Val<sup>447</sup> in the C $\mu$ 4 domain. Molecular modeling suggests that one of these loops essentially

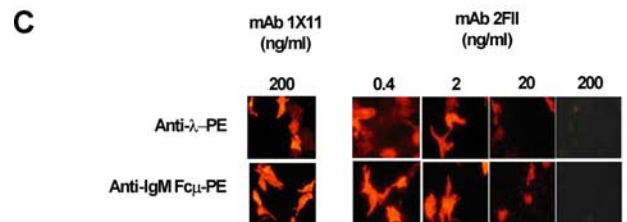
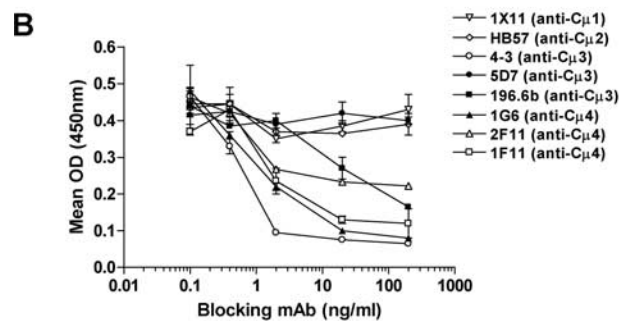
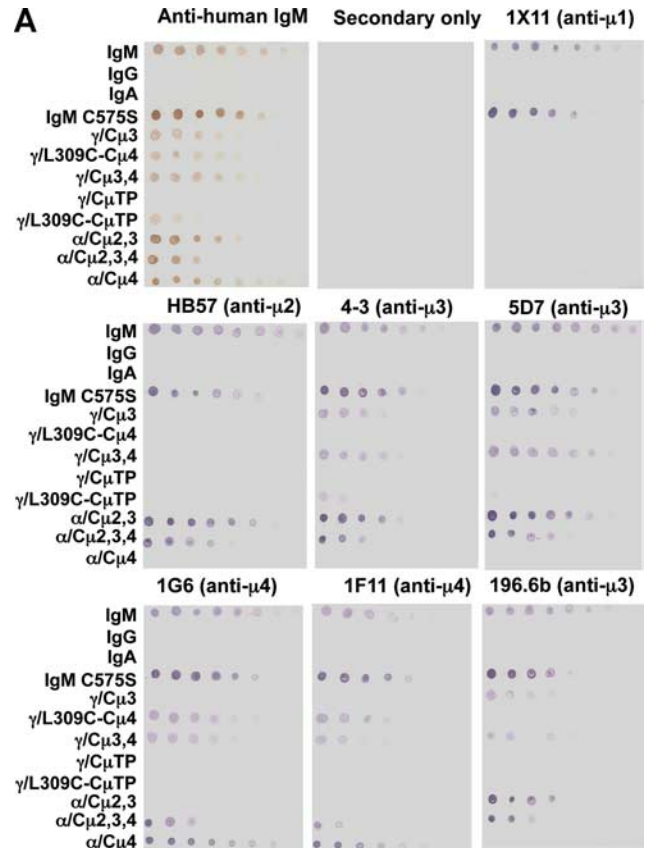


**FIGURE 6.** Epitope mapping of anti-human IgM mAbs and their effect on IgM binding to DBL4 $\beta$ . **A**, Domain-swapped and point-mutated Abs were serially diluted from left to right onto nitrocellulose membranes and blotted against a panel of anti-human IgM mAbs from a previous study (42, 43). mAbs 4-3, 5D7, and 196.6b bound to the C $\mu$ 3 domain, whereas mAbs 1F11 and 1G6 bound to the C $\mu$ 4 domain containing Abs. Binding of Abs was as for Western blots described in *Materials and Methods*. **B**, ELISA showing blocking of DBL4 $\beta$  binding to IgM by mAbs 4-3, 1G6, 1F11, 2F11, and 196.6. IgM was coated onto microtiter plates at 5  $\mu$ g/ml before incubation with varying concentrations of mAb. After washing, a fixed concentration of DBL4 $\beta$  (25  $\mu$ g/ml) was added and binding detected as described in *Materials and Methods*. **C**, Blocking of IgM binding to DBL4 $\beta$  COS-7 cell transfectants by mAb 2F11, in contrast with mAb 1X11, which was unable to block binding at equivalent concentrations (200 ng/ml), as seen in ELISAs. IgM binding was detected by anti- $\lambda$  (top panel) or anti-human Fc $\mu$  (bottom panel) PE-labeled Abs.

Table III. Binding of human IgM to infected erythrocytes of various *P. falciparum* isolates can be blocked by IgM Fc-specific mAbs<sup>a</sup>

mAb	Parasite Isolate				
	TM284	FCR3CSA	HB3R+	202CSA	HB3CSA
No mAb	23, 43, 25	35, 20	15, 48	34, 28	48
1X11 (C $\mu$ 1)	28, 36, 27	41, 21	16, 43	41, 39	49
4-3 (C $\mu$ 3)	2, 0, 0	0, 1	0, 0	0, 0	0
1F11 (C $\mu$ 4)	ND, 12, 4	11, 7	7, 16	12, 15	18
NHS	ND, ND, ND	ND, 22	ND, 51	32, 36	45

<sup>a</sup> Data represent percentage of parasitized erythrocytes binding human IgM by IFA in the presence or absence of each mAb. NHS indicates normal human serum control. Data typical of numerous experiments are shown.

occupies the analogous position to the *Staphylococcus aureus* protein A binding site on human IgG, and for the streptococcal IgA-binding proteins (Sir22 and Arp4) on human IgA (49). Since mouse IgM (this study) and bovine IgM do not bind the PfEMP1 variants and parasite strains investigated herein (27), we also made amino acid alignments of C $\mu$ 4 from different species and discovered that both mouse and bovine IgM differed from human IgM at two locations in the loops of interest (Fig. 5A). Therefore, we generated two human IgM mutants, termed PLSP394–397LLPQ and NR445–446HL, which, through replacement of Pro-Pro and Asn-Arg at positions 394–397 and 445–446, mimicked mouse IgM in these two exposed loops. Both mutations resulted in a complete loss of binding to DBL4 $\beta$  in ELISAs or IFAs (Fig. 5B) when used at equivalent concentrations to human IgM as determined by NIP-BSA-specific ELISAs (Fig. 5C). Intriguingly, these regions were also vital for the recognition of the C $\mu$ 4-specific mAb 2F11 (Fig. 5D) that also blocked binding of IgM to DBL4 $\beta$  (Fig. 6, B and C) and to parasitized RBC (data not shown). Size-exclusion chromatography revealed that both mutants ran predominantly as monomers when compared with either human IgM or the  $\gamma$ /L309C-C $\mu$ 4 mutant (Fig. 5E). Since it could be argued that the lack of binding by the two C $\mu$ 4 domain mutants arose because they existed principally as monomers, we enriched for pentamers by concentrating numerous fast protein liquid chromatography fractions containing the pentameric peak. Again, no binding of PLSP394–397LLPQ and NR445–446HL to DBL4 $\beta$  was observed in IFAs with transfected COS-7 cells.

#### Binding of PfEMP1 to IgM can be blocked with mAbs to the C $\mu$ 4 domain

To confirm the importance of the C $\mu$ 4 domain to PfEMP1 binding, we epitope mapped a panel of anti-IgM mAbs (Fig. 6A), previously used to investigate B cell receptor activation (42, 43). All the mAbs recognized human IgM but did not bind IgG or IgA (Fig. 6A). Epitope mapping of a panel of domain-swapped Abs revealed that mAbs 5D7, 4-3, and 196.6b bound to the C $\mu$ 3 domain, whereas mAbs 1F11, 1G6, and 2F11 (data not shown) bound to the C $\mu$ 4 domain. mAbs 1X11 and HB57 bind in the C $\mu$ 1 and C $\mu$ 2 domains, respectively (Fig. 6A), as observed previously and thereby they serve as useful negative controls (42, 43). Our finding that 5D7, 4-3, and 196.6b bind the C $\mu$ 3 domain rather than possessing C $\mu$ 4 specificity, as previously designated (42, 43), suggests that these mAbs may bind epitopes near the C terminus of the C $\mu$ 3 domain, potentially lost during tryptic digestion of IgM in the former analysis.

Preliminary incubation of IgM with the anti-C $\mu$ 4 mAbs (mAbs 1F11, 2F11, 1G6) could inhibit IgM binding to DBL4 $\beta$  when used at concentrations as low as 20 ng/ml (Figs. 6, B and C). Intriguingly, two anti-C $\mu$ 3 mAbs (196.6b and 4-3) could also block binding of human IgM, although higher concentrations of 196.6b were

required to achieve this effect than for 4-3, which consistently was the most inhibiting mAb (Figs. 6B and 7C). Both the C $\mu$ 3-specific mAb 4-3 and the C $\mu$ 4-specific mAb 1F11 significantly blocked binding of IgM to infected erythrocytes from various IgM-binding parasite isolates, whereas the C $\mu$ 1-specific mAb 1X11 did not (Table III). That mAb 1F11 was unable to completely inhibit IgM binding to infected erythrocytes when used at similar concentrations to mAb 4-3 fits with the known low affinity for IgM of this particular mAb (42, 43). These results indicate underlying similarity in the mechanism of IgM binding by multiple *P. falciparum* strains.

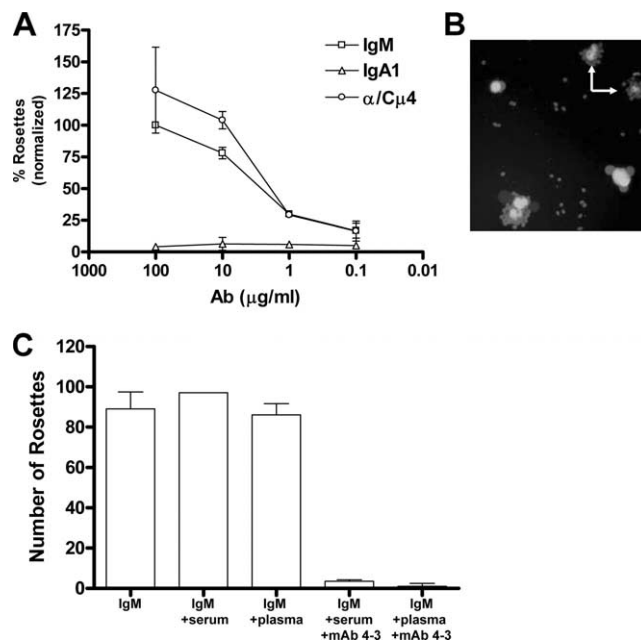


**FIGURE 7.** Development and disruption of pseudo-rosettes by C $\mu$ 4-specific mAbs. *A*, Binding of IgM, IgA1, or  $\alpha$ /C $\mu$ 4 Abs opsonized onto NIP-coated erythrocytes to DBL4 $\beta$ -transfected COS-7 cells assessed by pseudo-rosette formation. The results are normalized by expressing specific rosette formation as a percentage of that seen with erythrocytes coated with anti-NIP human IgM (Serotec) at 100  $\mu$ g/ml. *B*, The binding of Ab-coated erythrocytes to DBL4 $\beta$  transfectants (stained with acridine orange) to form rosettes (arrowed) were visualized by white light/fluorescence microscopy and a rosette defined as a DBL4 $\beta$ -transfected COS-7 cell surrounded by five or more erythrocytes. *C*, IgM-coated erythrocytes incubated in the presence of serum or plasma to allow opsonization and activation of components of the classical complement pathway still formed rosettes with DBL4 $\beta$  transfectants. Incubation of erythrocytes opsonized with IgM and complement components to mAb 4-3 totally blocked rosette formation.

### Functional analysis of the C $\mu$ 4 domain interaction with DBL4 $\beta$ and the role of complement

The ability of the  $\alpha$ /C $\mu$ 4 domain-swapped Ab to interact with DBL4 $\beta$ -transfected COS-7 cells was also assessed by pseudo-rosetting assays (Fig. 7). As expected, IgM or the  $\alpha$ /C $\mu$ 4 domain swap, when opsonized onto NIP-coated erythrocytes could rosette to DBL4 $\beta$ -expressing COS-7 cells with an affinity comparable to that of known Fc-FcR interactions (Figs. 7, A and B, arrows). A control dimeric IgA1 was unable to form rosettes with DBL4 $\beta$ -expressing COS-7 cells as expected. Intriguingly, IgM-opsonized erythrocytes that were incubated in serum or plasma as a source of complement or purified C1q (data not shown) were still capable of forming rosettes with DBL4 $\beta$ -transfected COS-7 cells (Fig. 7C), allowing us to conclude that the presence of members of the classical pathway, deposited on and around IgM, do not occlude the binding site for DBL4 $\beta$  in the C $\mu$ 4 domain. As predicted from our IFA data, the C $\mu$ 3-specific blocking mAb 4-3 completely inhibited rosette formation between IgM-coated erythrocytes and the DBL4 $\beta$ -expressing COS-7 cells, even in the presence of deposited complement components (Fig. 7C).

## Discussion

PfEMP1 is a multiligand receptor expressed on the surface of infected erythrocytes that is responsible for parasite virulence phenotypes in African children, such as rosetting, and sequestration to the placenta in women (30, 50). PfEMP1 is composed of cysteine-rich domains known as DBL domains that play a key role in malaria pathogenesis by mediating adhesion to human cells (51). Herein we have identified the PfEMP1 variant transcribed by rosetting parasites from the strain TM284 (encoded by the *TM284var1* gene) and show that a specific domain from this PfEMP1 variant (DBL4 $\beta$ ) binds to human IgM. We then used this *P. falciparum* IgM-binding protein as a tool to investigate the detailed mechanism of interaction between PfEMP1 and human IgM.

To analyze regions on IgM critical for the interaction with DBL4 $\beta$ , we employed domain-swapped Abs and point mutants (Fig. 2). As discussed previously (37, 38), these mutant proteins are unlikely to have undergone any gross structural aberrations, allowing conclusions to be drawn on the relative contributions of different domains and mutated residues of IgM to the binding of PfEMP1. Our results indicate that DBL4 $\beta$ , whether expressed in *E. coli* or when presented on the surface of mammalian cell lines, binds to the Fc portion of the IgM H chain, and requires the C $\mu$ 4 domain (Figs. 3–5). The binding of PfEMP1 to IgM was crucially dependent on the polymeric nature of IgM, since both Fabs and monomeric versions of IgM failed to bind (Fig. 4). This finding is in agreement with previous work showing that IgM monomers do not increase the size of rosettes when added back to IgM-depleted serum (15). Although the affinity of an individual DBL domain for IgM may be low, the pentameric nature of IgM allows for an increased avidity, allowing significant cell-to-cell interactions as observed in our functional pseudo-rosetting assays using Ig-coated erythrocytes and DBL4 $\beta$  expressed in COS-7 cells (Fig. 7).

Importantly, the above results with a single PfEMP1 domain were also mirrored in experiments using the domain-swapped Abs in IFAs with live infected erythrocytes of strains TM284 (rosetting) and FCR3CSA (CSA binding) (Table II). Furthermore, experiments using mAbs specific for different regions of the IgM H chain (Fig. 6) showed a similar pattern of inhibition

of IgM-binding in five distinct parasite strains (two rosetting and three CSA binding) (Table III). This suggests that diverse parasite isolates expressing distinct PfEMP1 variants (this study and Ref. 27) all bind to the same (or similar) sites on the human IgM molecule. Given the diversity in different PfEMP1 domains implicated in IgM binding (outlined in detail in the *Introduction*), this homogeneity among strains in binding to a particular site on IgM is unexpected, and may indicate that this site plays an important role in the host-parasite interaction. It will also be important to determine whether the affinity for IgM seen by DBL domains from rosetting (non-CSA-binding) parasites is similar to that for DBL domains from nonrosetting (and CSA-binding) isolates. Future work should also address if there is a common IgM interaction site on these diverse *P. falciparum* DBL domains. Recent findings suggest that diverse DBL $\beta$ -C2 domains from numerous isolates use an equivalent glycan-binding region when binding ICAM-1, implying a general model for how DBL domains evolve under dual selection for host receptor binding and immune evasion (52).

We were able to localize some of the amino acid residues within the IgM C $\mu$ 4 domain that are of particular importance in PfEMP1 binding (Fig. 5), including the PNRV (residues 444–447) and PLSP (residues 394–397) loops, predicted to lie on the surface of the C $\mu$ 4 domain (Fig. 8). Intriguingly, the PNRV loop is homologous to regions on both IgG and IgA responsible for binding to bacterial Fc-binding proteins (49). Since natural selection has shaped the interaction of the Fc region of Abs with bacterial decoy proteins, the possibility exists that this area on IgM has also been selected for by parasitism (53). Given the overlapping nature of the binding sites in IgA-Fc for Fc $\alpha$ R1 (CD89) and bacterial IgA-binding proteins (41, 49, 54), it could be postulated that this region is important for IgM function, and that it is in some way beneficial for the infected erythrocyte to block it. Ongoing work in our laboratories has shown that those mAbs that inhibited binding to DBL4 $\beta$  also prevented binding of IgM to the Fc $\alpha$ / $\mu$ R, suggesting that the binding site for the two ligands lie close to each other. However, the interaction with Fc $\alpha$ / $\mu$ R does require additional and unique contacts, since the  $\gamma$ /L309C-C $\mu$ 4 domain swap shown to bind to DBL4 $\beta$  in this study did not bind Fc $\alpha$ / $\mu$ R; and mouse IgM, shown not to bind DBL4 $\beta$ , was capable of binding Fc $\alpha$ / $\mu$ R (A. Ghumra, R. S. McIntosh, I. Sandlie, F.-E. Johansen, P. K. Mongini, and R. J. Pleass, unpublished data). Furthermore, the extracellular portion of the pIgR (free secretory component) previously shown to bind the Fc of IgM failed to prevent IgM binding to DBL4 $\beta$ . However, free secretory component did compete out binding of IgM to Fc $\alpha$ / $\mu$ R, supporting our notion that unique contacts are involved for binding of IgM to either Fc $\alpha$ / $\mu$ R or the pIgR (Ref. 40 and A. Ghumra, R. S. McIntosh, I. Sandlie, F.-E. Johansen, P. K. Mongini, and R. J. Pleass, unpublished data). Future experiments will address the ability of IgM bound to PfEMP1 to interact with functionally important host receptors for IgM, such as Fc $\alpha$ / $\mu$ R and the pIgR (3, 40).

Further work will also be needed to investigate the effect of IgM binding by PfEMP1 on the ability of IgM to activate complement. The possible involvement of complement in IgM binding and rosette formation is particularly intriguing given the evidence that complement receptor 1 (CR1) is a rosette formation receptor on uninfected erythrocytes (30), and CR1 interacts with *P. falciparum*-infected cells via its C3b binding sites (55). Existing data suggest that complement activation is not required for rosette formation because rosettes form normally in C3- and C4-deficient

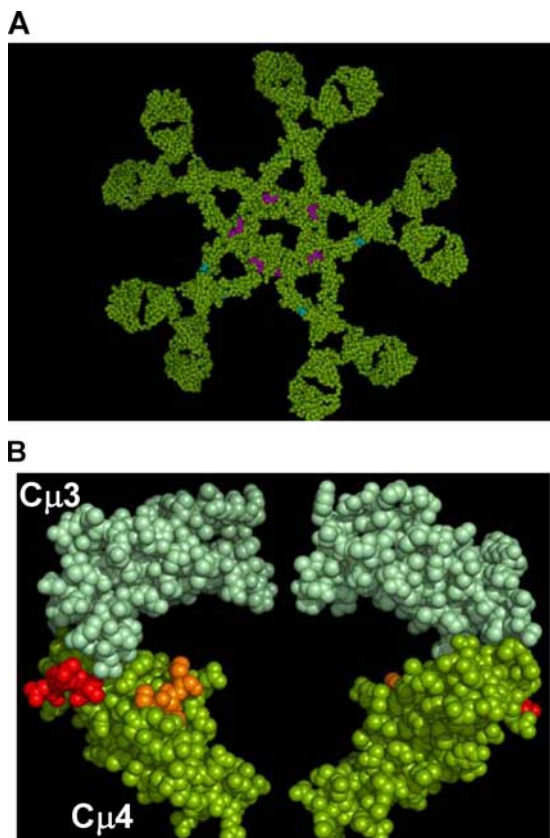


**FIGURE 8.** Molecular models of human IgM highlighting residues interacting with Fc-binding proteins. *A*, Model of human IgM (kindly provided by Professor Stephen Perkins, University College, University of London) annotating sites in the  $C\mu 4$  domain involved in DBL4 $\beta$  binding and sites in the  $C\mu 3$  domain important for interaction with C1q (turquoise) (2). *B*, Molecular model (generated by PyMOL) showing the two sides of IgM-Fc based on the known crystal structure of the analogous IgE-Fc (100V.pdb) (62). Exposed highlighted residues Pro<sup>394</sup>-Pro<sup>397</sup> (orange) and Pro<sup>444</sup>-Val<sup>447</sup> (red) in the  $C\mu 4$  domain have been shown to be involved in the interaction with DBL4 $\beta$ . The C-terminal tailpieces are omitted for clarity.

human sera (55). However, a role for other complement components in rosetting has not been excluded. C1q is a possible candidate for involvement in rosetting because it is known to bind to the  $C\mu 3$  domain of IgM-Fc with high affinity (2), and it is also known to interact with CR1 (Fig. 8 and Ref. 56). We therefore investigated whether C1q influenced the interaction between IgM and PfEMP1 using pseudo-rosetting assays in which Ig-coated erythrocytes were incubated with COS-7 cells expressing the IgM-binding PfEMP1 domain DBL4 $\beta$  (Fig. 7). In these pseudo-rosetting assays, IgM would be bound to the erythrocyte in its “crab-like” formation, thus exposing the C1q binding sites in the  $C\mu 3$  domain. Despite the presence of saturating levels of complement, it was clear that IgM could still interact with DBL4 $\beta$  (Fig. 7). However, the epitope on the Fc of IgM seen by the blocking mAbs (and presumably DBL4 $\beta$ ) is still exposed since these could completely block rosette formation even in the presence of saturating levels of complement. These findings allow us to postulate a number of structural explanations for how complement inactivation might be achieved by the infected erythrocyte for parasite-specific IgM. Recent structural models of the C1 complex have shown that both C1r and C1s, required for activation of the classical pathway, bind in the middle of the cone defined by the C1q stems, where they occupy a large area sitting over the  $C\mu 4$  domains of IgM (57). It

is therefore possible that DBL4 $\beta$  bound to the  $C\mu 4$  domain of IgM may interfere with complement activation. An alternative and simpler explanation for the known complement resistance of infected erythrocytes is that parasite-specific IgM bound to the surface of the parasitized red cell undergoes a conformational change on binding pertinent DBL domains, which re-closes the C1q binding site in the  $C\mu 3$  domain, thereby blocking access to C1q. We are currently developing recombinant human IgM molecules with specificity for different DBL domains, including DBL4 $\beta$ , to investigate these possibilities. The tools described herein will be critical to such analyses.

Rosetting and placental parasite isolates may also bind nonspecific IgM to allow masking of critical PfEMP1 domains from the destructive action of specific Abs. However, we were unable to substantiate this hypothesis since DBL4 $\beta$ -specific IgG responses were not detectable in a cohort of immune Gambian plasma available to us (58). However, the DBL4 $\beta$  domain described in this work was derived from TM284, a Thai isolate potentially expressing antigenically distinct PfEMP1 epitopes compared with Gambian parasites. It will be interesting to assess the effect of DBL4 $\beta$  specific antisera derived in immunization studies on IgM binding. The work herein focuses on IgM binding by PfEMP1; however, the experiments do also shed further light on a recent controversy over whether infected erythrocytes can also bind nonimmune IgG. Some previous reports suggest that IgM-binding *P. falciparum* strains can also bind IgG from normal human serum (14, 18, 26). However, we have consistently been unable to detect nonimmune IgG binding by any *P. falciparum* rosetting or CSA-binding strain using multiple different detection reagents (10, 17). Although only experiments using identical parasite lines used by others will completely rule out nonspecific IgG binding, the results herein indicate that IgM binding is determined both by specific amino acids within IgM and by the polymeric nature of normal IgM molecules. IgG did not bind to infected erythrocytes, even when an artificial polymeric form of IgG was tested (Table II and Fig. 4). The experiments that we conducted here with IgG/IgM domain-swapped Abs would not have been possible if *P. falciparum* did bind nonimmune IgG. One other controversy in the literature concerns the ability of IgM-binding strains to bind mouse IgM. We reported previously that mouse IgM does bind to the surface of infected erythrocytes (17); however, these experiments relied on the use of chloroquine to elute human IgM (derived from the parasite culture medium) from the surface of infected erythrocytes before incubation with mouse IgM. In the present study we used infected erythrocytes grown in human IgM-depleted serum and found that mouse IgM did not bind. It may be that the high concentrations of chloroquine used in our previous study had adverse effects on membrane function and gave misleading results.

In summary, we have demonstrated that PfEMP1 binds to the  $C\mu 4$  domain of human IgM and that this mechanism is shared by diverse *P. falciparum* strains. These findings have allowed us to propose a possible mechanism by which PfEMP1 molecules may bind IgM and simultaneously interact with other serum proteins. Since PfEMP1 from both rosetting and placental isolates binds in the same region of IgM, specific inhibitors of the interaction may prove useful in diverse clinical settings.

### Acknowledgments

We thank Professor Tor Lea of the Institute of Immunology, Rikshospitalet, Oslo, Norway, for providing mAb 2F11, and Professor Paul Morgan and Drs. Jenny Woof and Melanie Lewis for useful discussions on complement assays. We also thank Kelly-Ann Vere for help with confocal microscopy and Drs. Karen Bunting and Jody Winter for assistance in

expressing various DBL domains in *E. coli*. We also thank Professor Steve Perkins for kindly providing an  $\alpha$ -carbon trace of IgM.

## Disclosures

The authors have no financial conflicts of interest.

## References

- Burton, D. R. 1987. Structure and function of antibodies. In *Molecular Genetics of Immunoglobulin*. F. Calabi and M. S. Neuberger, eds. Elsevier Science (Biomedical Division), Amsterdam, pp. 1–49.
- Perkins, S. J., A. S. Nealis, B. J. Sutton, and A. Feinstein. 1991. Solution structure of human and mouse immunoglobulin M by synchrotron X-ray scattering and molecular graphics modelling: a possible mechanism for complement activation. *J. Mol. Biol.* 221: 1345–1366.
- Shibuya, A., N. Sakamoto, Y. Shimizu, K. Shibuya, M. Osawa, T. Hiroshima, H. J. Eyre, G. R. Sutherland, Y. Endo, T. Fujita, et al. 2000. Fc $\alpha$ / $\mu$  receptor mediates endocytosis of IgM-coated microbes. *Nat. Immunol.* 1: 441–446.
- Sakamoto, N., K. Shibuya, Y. Shimizu, K. Yotsumoto, T. Miyabayashi, S. Sakano, T. Tsuji, E. Nakayama, H. Nakauchi, and A. Shibuya. 2001. A novel Fc receptor for IgA and IgM is expressed on both hematopoietic and non-hematopoietic tissues. *Eur. J. Immunol.* 31: 1310–1316.
- Cho, Y., K. Usui, S. Honda, S. Tahara-Hanaoka, K. Shibuya, and A. Shibuya. 2006. Molecular characteristics of IgA and IgM Fc binding to the Fc $\alpha$ / $\mu$ R. *Biochem. Biophys. Res. Commun.* 345: 474–478.
- Harte, P. G., A. Cooke, and J. H. Playfair. 1983. Specific monoclonal IgM is a potent adjuvant in murine malaria vaccination. *Nature* 302: 256–258.
- Couper, K. N., R. S. Phillips, F. Brombacher, and J. Alexander. 2005. Parasite-specific IgM plays a significant role in the protective immune response to asexual erythrocytic stage *Plasmodium chabaudi* AS infection. *Parasite Immunol.* 27: 171–180.
- Ochsenbein, A. F., F. Fehr, C. Lutz, M. Suter, F. Brombacher, H. Hengartner, and R. M. Zinkernagel. 1999. Control of early viral and bacterial distribution and disease by natural antibodies. *Science* 286: 2156–2159.
- Boes, M., A. P. Prodeus, T. Schmidt, M. C. Carroll, and J. Chen. 1998. A critical role of natural immunoglobulin M in immediate defense against systemic bacterial infection. *J. Exp. Med.* 188: 2381–2386.
- Rowe, J. A., J. Shafi, O. K. Kai, K. Marsh, and A. Raza. 2002. Non-immune IgM, but not IgG binds to the surface of *Plasmodium falciparum*-infected erythrocytes and correlates with rosetting and severe malaria. *Am. J. Trop. Med. Hyg.* 66: 692–699.
- Carlson, J., H. Helmby, A. V. Hill, D. Brewster, B. M. Greenwood, and M. Wahlgren. 1990. Human cerebral malaria: association with erythrocyte rosetting and lack of anti-rosetting antibodies. *Lancet* 336: 1457–1460.
- Rowe, J. A., J. Obeiro, C. I. Newbold, and K. Marsh. 1995. *Plasmodium falciparum* rosetting is associated with malaria severity in Kenya. *Infect. Immun.* 63: 2323–2326.
- Clough, B., F. A. Atilola, J. Black, and G. Pasvol. 1998. *Plasmodium falciparum*: the importance of IgM in the rosetting of parasite-infected erythrocytes. *Exp. Parasitol.* 89: 129–132.
- Scholander, C., C. J. Treutiger, K. Hulthenby, and M. Wahlgren. 1996. Novel fibrillar structure confers adhesive property to malaria-infected erythrocytes. *Nat. Med.* 2: 204–208.
- Sommer, E. A., J. Black, and G. Pasvol. 2000. Multiple human serum components act as bridging molecules in rosette formation by *Plasmodium falciparum*-infected erythrocytes. *Blood* 95: 674–682.
- Treutiger, C. J., C. Scholander, J. Carlson, K. P. McAdam, J. G. Raynes, L. Falksveden, and M. Wahlgren. 1999. Rouleaux-forming serum proteins are involved in the rosetting of *Plasmodium falciparum*-infected erythrocytes. *Exp. Parasitol.* 93: 215–224.
- Creasey, A. M., T. Staalsoe, A. Raza, D. E. Arnot, and J. A. Rowe. 2003. Non-specific immunoglobulin M binding and chondroitin sulfate A binding are linked phenotypes of *Plasmodium falciparum* isolates implicated in malaria during pregnancy. *Infect. Immun.* 71: 4767–4771.
- Rasti, N., F. Namusoke, A. Chêne, Q. Chen, T. Staalsoe, M. Q. Klinkert, F. Mirembé, F. Kironde, and M. Wahlgren. 2006. Non-immune immunoglobulin binding and multiple adhesion characterize *Plasmodium falciparum*-infected erythrocytes of placental origin. *Proc. Natl. Acad. Sci. USA* 103: 13795–13800.
- Nezlin, R., and V. Ghetie. 2004. Interactions of immunoglobulins outside the antigen-combining site. *Adv. Immunol.* 82: 155–215.
- Baruch, D. I., B. L. Pasloske, H. B. Singh, X. Bi, X. C. Ma, M. Feldman, T. F. Taraschi, and R. J. Howard. 1995. Cloning the *P. falciparum* gene encoding PfEMP1, a malarial variant antigen and adherence receptor on the surface of parasitized human erythrocytes. *Cell* 82: 77–87.
- Smith, J. D., C. E. Chitnis, A. G. Craig, D. J. Roberts, D. E. Hudson-Taylor, D. S. Peterson, R. Pinches, C. I. Newbold, and L. H. Miller. 1995. Switches in expression of *Plasmodium falciparum* var genes correlate with changes in antigenic and cytoadherent phenotypes of infected erythrocytes. *Cell* 82: 101–110.
- Kyes, S. A., S. M. Kraemer, and J. D. Smith. 2007. Antigenic variation in *Plasmodium falciparum*: gene organization and regulation of the var multigene family. *Eukaryot. Cell* 6: 1511–1520.
- Gardner, M. J., N. Hall, E. Fung, O. White, M. Berriman, R. W. Hyman, J. M. Carlton, A. Pain, K. E. Nelson, S. Bowman, et al. 2002. Genome sequence of the human malaria parasite *Plasmodium falciparum*. *Nature* 419: 498–511.
- Smith, J. D., G. Subramanian, B. Gamain, D. I. Baruch, and L. H. Miller. 2000. Classification of adhesive domains in the *Plasmodium falciparum* erythrocyte membrane protein 1 family. *Mol. Biochem. Parasitol.* 110: 293–310.
- Chen, Q., A. Heddini, A. Barragan, V. Fernandez, S. F. Pearce, and M. Wahlgren. 2000. The semi-conserved head structure of *Plasmodium falciparum* erythrocyte membrane protein 1 mediates binding to multiple independent host receptors. *J. Exp. Med.* 192: 1–10.
- Flick, K., C. Scholander, Q. Chen, V. Fernandez, B. Povellet, J. Gysin, and M. Wahlgren. 2001. Role of non-immune IgG bound to PfEMP1 in placental malaria. *Science* 293: 2098–2100.
- Semblat, J. P., A. Raza, S. A. Kyes, and J. A. Rowe. 2006. Identification of *Plasmodium falciparum* var1CSA and var2CSA domains that bind IgM natural antibodies. *Mol. Biochem. Parasitol.* 146: 192–197.
- Rowe, J. A., A. R. Berendt, K. Marsh, and C. I. Newbold. 1994. *Plasmodium falciparum*: a family of sulphated glycoconjugates disrupts erythrocyte rosettes. *Exp. Parasitol.* 79: 506–516.
- Carlson, J., and M. Wahlgren. 1992. *Plasmodium falciparum* erythrocyte rosetting is mediated by promiscuous lectin-like interactions. *J. Exp. Med.* 176: 1311–1317.
- Rowe, J. A., J. M. Moulds, C. I. Newbold, and L. H. Miller. 1997. *P. falciparum* rosetting mediated by a parasite-variant erythrocyte membrane protein and complement-receptor 1. *Nature* 388: 292–295.
- Kyes, S. A., R. Pinches, and C. I. Newbold. 2000. A simple RNA analysis method shows var and rif multigene family expression patterns in *Plasmodium falciparum*. *Mol. Biochem. Parasitol.* 105: 311–315.
- Taylor, H. M., S. A. Kyes, D. Harris, N. Kriek, and C. I. Newbold. 2000. A study of var gene transcription in vitro using universal var gene primers. *Mol. Biochem. Parasitol.* 105: 12–23.
- Kyriacou, H. M., G. N. Stone, R. J. Challis, A. Raza, K. E. Lyke, M. A. Thera, A. K. Koné, O. K. Doumbo, C. V. Plowe, and J. A. Rowe. 2006. Differential var gene transcription in *Plasmodium falciparum* isolates from patients with cerebral malaria compared to hyperparasitaemia. *Mol. Biochem. Parasitol.* 150: 211–218.
- Cohen, G. H., W. C. Wilcox, D. L. Sadora, D. Long, J. Z. Levin, and R. J. Eisenberg. 1988. Expression of herpes simplex virus type 1 glycoprotein D deletion mutants in mammalian cells. *J. Virol.* 62: 1932–1940.
- Chitnis, C. E., and L. H. Miller. 1994. Identification of the erythrocyte binding domains of *Plasmodium vivax* and *Plasmodium knowlesi* proteins involved in erythrocyte invasion. *J. Exp. Med.* 180: 497–506.
- Singh, S. K., A. P. Singh, S. Pandey, S. S. Yazdani, C. E. Chitnis, and A. Sharma. 2003. Definition of structural elements in *Plasmodium vivax* and *P. knowlesi* Duffy-binding domains necessary for erythrocyte invasion. *Biochem. J.* 374: 193–198.
- Sørensen, V., I. B. Rasmussen, L. Norderhaug, I. Natvig, T. E. Michaelsen, and I. Sandlie. 1996. Effect of the IgM and IgA secretory tailpieces on polymerization and secretion of IgM and IgG. *J. Immunol.* 156: 2858–2865.
- Sørensen, V., V. Sundvold, T. E. Michaelsen, and I. Sandlie. 1999. Polymerization of IgA and IgM: roles of Cys309/Cys414 and the secretory tailpiece. *J. Immunol.* 162: 3448–3455.
- Sørensen, V., I. B. Rasmussen, V. Sundvold, T. E. Michaelsen, and I. Sandlie. 2000. Structural requirements for incorporation of J chain into human IgM and IgA. *Int. Immunol.* 12: 19–27.
- Braathén, R., V. Sørensen, P. Brandtzaeg, I. Sandlie, and F. E. Johansen. 2002. The carboxyl-terminal domains of IgA and IgM direct isotype-specific polymerization and interaction with the polymeric immunoglobulin receptor. *J. Biol. Chem.* 277: 42755–42762.
- Pleass, R. J., J. I. Dunlop, C. M. Anderson, and J. M. Woof. 1999. Identification of residues in the CH2/CH3 domain interface of IgA essential for interaction with the human Fc $\alpha$  receptor (Fc $\alpha$ R) CD89. *J. Biol. Chem.* 274: 23508–23514.
- Rudich, S. M., R. Winchester, and P. K. Mongini. 1985. Human B-cell activation: evidence for diverse signals provided by various monoclonal anti-IgM antibodies. *J. Exp. Med.* 162: 1236–1255.
- Rudich, S. M., E. Mihaesco, R. Winchester, and P. K. Mongini. 1987. Analysis of the domain specificity of various murine anti-human IgM monoclonal antibodies differing in human B-lymphocyte signaling activity. *Mol. Immunol.* 24: 809–820.
- Duffy, M. F., G. V. Brown, W. Basuki, E. O. Krejany, R. Noviyanti, A. F. Cowman, and J. C. Reeder. 2002. Transcription of multiple var genes by individual, trophozoite-stage *Plasmodium falciparum* cells expressing a chondroitin-sulphate A binding phenotype. *Mol. Microbiol.* 43: 1285–1293.
- Kaestli, M., I. A. Cockburn, A. Cortés, K. Baea, J. A. Rowe, and H. P. Beck. 2006. Virulence of malaria is associated with differential expression of *Plasmodium falciparum* var gene subgroups in a case-control study. *J. Infect. Dis.* 193: 1567–1574.
- Jensen, A. T., P. Magistrado, S. Sharp, L. Joergensen, T. Lavstsen, A. Chiuchiuini, A. Salanti, L. S. Vestergaard, J. P. Lusingu, R. Hermesen, et al. 2004. *Plasmodium falciparum* associated with severe childhood malaria preferentially expresses PfEMP1 encoded by group A var genes. *J. Exp. Med.* 199: 1179–1190.
- Davis, A. C., C. Collins, M. I. Yoshimura, G. D'Agostaro, and M. J. Shulman. 1989. Mutations of the mouse mu H chain which prevent polymer assembly. *J. Immunol.* 143: 1352–1357.
- Sitia, R., M. Neuberger, C. Alberini, P. Bet, A. Fra, G. Valetti, C. Williams, and C. Milstein. 1990. Developmental regulation of IgM secretion: the role of the carboxy-terminal cysteine. *Cell* 60: 781–790.
- Pleass, R. J., T. Areschoug, G. Lindahl, and J. M. Woof. 2001. Streptococcal IgA-binding proteins bind in the Ca $^{2+}$ -Ca $^{3+}$  interdomain region and inhibit binding of IgA to human CD89. *J. Biol. Chem.* 276: 8197–8204.
- Rowe, J. A., and S. A. Kyes. 2004. The role of *Plasmodium falciparum* var genes in malaria in pregnancy. *Mol. Microbiol.* 53: 1011–1019.

51. Howell, D. P., R. Samudrala, and J. D. Smith. 2006. Disguising itself: insights into *Plasmodium falciparum* binding and immune evasion from the DBL crystal structure. *Mol. Biochem. Parasitol.* 148: 1–9.
52. Howell, D. P., E. A. Levin, A. L. Springer, S. M. Kraemer, D. J. Phippard, W. R. Schief, and J. D. Smith. 2007. Mapping a common interaction site used by *Plasmodium falciparum* Duffy binding-like domains to bind diverse host receptors. *Mol. Microbiol.* 67: 78–87.
53. Abi-Rached, L., K. Dorigi, P. J. Norman, M. Yawata, and P. Parham. 2007. Episodes of natural selection shaped the interactions of IgA-Fc with Fc $\alpha$ RI and bacterial decoy proteins. *J. Immunol.* 178: 7943–7954.
54. Ramsland, P. A., N. Willoughby, H. M. Trist, W. Farrugia, P. M. Hogarth, J. D. Fraser, and B. D. Wines. 2007. Structural basis for evasion of IgA immunity by *Staphylococcus aureus* revealed in the complex of SSL7 with Fc of human IgA1. *Proc. Natl. Acad. Sci. USA* 104: 15051–15056.
55. Rowe, A. J., S. J. Rogerson, A. Raza, J. M. Moulds, M. D. Kazatchkine, K. Marsh, C. I. Newbold, J. P. Atkinson, and L. H. Miller. 2000. Mapping of the region of complement receptor (CR) 1 required for *P. falciparum* rosetting and demonstration of the importance of CR1 in rosetting in field isolates. *J. Immunol.* 165: 6341–6346.
56. Tas, S. W., L. B. Klickstein, S. F. Barbashov, and A. Nicholson-Weller. 1999. C1q and C4b bind simultaneously to CR1 and additively support erythrocyte adhesion. *J. Immunol.* 163: 5056–5063.
57. Gaboriaud, C., N. M. Thielens, L. A. Gregory, V. Rossi, J. C. Fontecilla-Camps, and G. J. Arlaud. 2004. Structure and activation of the C1 complex of complement: unraveling the puzzle. *Trends Immunol.* 25: 368–373.
58. Corran, P. H., R. A. O'Donnell, J. Todd, C. Uthaipibull, A. A. Holder, B. S. Crabb, and E. M. Riley. 2004. The fine specificity, but not the invasion inhibitory activity, of 19-kilodalton merozoite surface protein 1-specific antibodies is associated with resistance to malarial parasitemia in a cross-sectional survey in The Gambia. *Infect. Immun.* 72: 6185–6189.
59. Putnam, F. W., Y. S. Liu, and T. L. Low. 1979. Primary structure of a human IgA1 immunoglobulin: IV. Streptococcal IgA1 protease, digestion, Fab and Fc fragments, and the complete amino acid sequence of the alpha 1 heavy chain. *J. Biol. Chem.* 254: 2865–2874.
60. Wiersma, E. J., and M. J. Shulman. 1995. Assembly of IgM: the role of disulfide bonding and non-covalent interactions. *J. Immunol.* 154: 5265–5272.
61. Kabat, E. A., T. T. Wu, M. Reid-Miller, H. Perry, and K. S. Gottesman. 1987. *Sequences of Proteins of Immunological Interest*, 4th Ed. U.S. Department of Health and Human Services, National Institutes of Health, Washington D.C.
62. Wan, T., R. L. Beavil, S. M. Fabiane, A. J. Beavil, M. K. Sohi, M. Keown, R. J. Young, A. J. Henry, R. J. Owens, H. J. Gould, and B. J. Sutton. 2002. The crystal structure of IgE Fc reveals an asymmetrically bent conformation. *Nat. Med.* 3: 681–686.